



Hydrodynamic instability growth and mix experiments at the National Ignition Facility)

V. A. Smalyuk, M. Barrios, J. A. Caggiano, D. T. Casey, C. J. Cerjan, D. S. Clark, M. J. Edwards, J. A. Frenje, M. Gatu-Johnson, V. Y. Glebov, G. Grim, S. W. Haan, B. A. Hammel, A. Hamza, D. E. Hoover, W. W. Hsing, O. Hurricane, J. D. Kilkenny, J. L. Kline, J. P. Knauer, J. Kroll, O. L. Landen, J. D. Lindl, T. Ma, J. M. McNaney, M. Mintz, A. Moore, A. Nikroo, T. Parham, J. L. Peterson, R. Petrasso, L. Pickworth, J. E. Pino, K. Raman, S. P. Regan, B. A. Remington, H. F. Robey, D. P. Rowley, D. B. Sayre, R. E. Tipton, S. V. Weber, K. Widmann, D. C. Wilson, and C. B. Yeamans

Citation: *Physics of Plasmas* (1994-present) **21**, 056301 (2014); doi: 10.1063/1.4872026

View online: <http://dx.doi.org/10.1063/1.4872026>

View Table of Contents: <http://scitation.aip.org/content/aip/journal/pop/21/5?ver=pdfcov>

Published by the *AIP Publishing*

Articles you may be interested in

[Detailed implosion modeling of deuterium-tritium layered experiments on the National Ignition Facility\)](#)
Phys. Plasmas **20**, 056318 (2013); 10.1063/1.4802194

[Solid debris collection for radiochemical diagnostics at the National Ignition Facility\)](#)
Rev. Sci. Instrum. **83**, 10D904 (2012); 10.1063/1.4732856

[Cryogenic thermonuclear fuel implosions on the National Ignition Facility\)](#)
Phys. Plasmas **19**, 056318 (2012); 10.1063/1.4719686

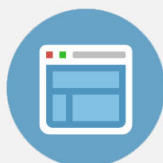
[Diagnosing ignition with DT reaction history\)](#)
Rev. Sci. Instrum. **79**, 10E525 (2008); 10.1063/1.2969420

[Implosion hydrodynamics of fast ignition targets\)](#)
Phys. Plasmas **12**, 056312 (2005); 10.1063/1.1896952



Re-register for Table of Content Alerts

Create a profile.



Sign up today!



Hydrodynamic instability growth and mix experiments at the National Ignition Facility^{a)}

V. A. Smalyuk,^{1,b)} M. Barrios,¹ J. A. Caggiano,¹ D. T. Casey,¹ C. J. Cerjan,¹ D. S. Clark,¹ M. J. Edwards,¹ J. A. Frenje,² M. Gatu-Johnson,² V. Y. Glebov,³ G. Grim,⁴ S. W. Haan,¹ B. A. Hammel,¹ A. Hamza,¹ D. E. Hoover,⁵ W. W. Hsing,¹ O. Hurricane,¹ J. D. Kilkenny,⁵ J. L. Kline,⁴ J. P. Knauer,³ J. Kroll,¹ O. L. Landen,¹ J. D. Lindl,¹ T. Ma,¹ J. M. McNaney,¹ M. Mintz,¹ A. Moore,⁶ A. Nikroo,⁵ T. Parham,¹ J. L. Peterson,¹ R. Petrasso,² L. Pickworth,¹ J. E. Pino,¹ K. Raman,¹ S. P. Regan,³ B. A. Remington,¹ H. F. Robey,¹ D. P. Rowley,¹ D. B. Sayre,¹ R. E. Tipton,¹ S. V. Weber,¹ K. Widmann,¹ D. C. Wilson,⁴ and C. B. Yeamans¹

¹Lawrence Livermore National Laboratory, NIF Directorate, Livermore, California 94550, USA

²Massachusetts Institute of Technology, Cambridge, Massachusetts 02139, USA

³Laboratory for Laser Energetics, University of Rochester, Rochester, New York 14623, USA

⁴Los Alamos National Laboratory, Los Alamos, New Mexico 97544, USA

⁵General Atomics, San Diego, California 92186, USA

⁶AWE Aldermaston, Reading, Berkshire RG7 4PR, United Kingdom

(Received 6 December 2013; accepted 14 January 2014; published online 22 April 2014)

Hydrodynamic instability growth and its effects on implosion performance were studied at the National Ignition Facility [G. H. Miller, E. I. Moses, and C. R. Wuest, *Opt. Eng.* **443**, 2841 (2004)]. Implosion performance and mix have been measured at peak compression using plastic shells filled with tritium gas and containing embedded localized carbon-deuterium diagnostic layers in various locations in the ablator. Neutron yield and ion temperature of the deuterium-tritium fusion reactions were used as a measure of shell-gas mix, while neutron yield of the tritium-tritium fusion reaction was used as a measure of implosion performance. The results have indicated that the low-mode hydrodynamic instabilities due to surface roughness were the primary culprits for yield degradation, with atomic ablator-gas mix playing a secondary role. In addition, spherical shells with pre-imposed 2D modulations were used to measure instability growth in the acceleration phase of the implosions. The capsules were imploded using ignition-relevant laser pulses, and ablation-front modulation growth was measured using x-ray radiography for a shell convergence ratio of ~ 2 . The measured growth was in good agreement with that predicted, thus validating simulations for the fastest growing modulations with mode numbers up to 90 in the acceleration phase. Future experiments will be focused on measurements at higher convergence, higher-mode number modulations, and growth occurring during the deceleration phase. © 2014 AIP Publishing LLC.

[<http://dx.doi.org/10.1063/1.4872026>]

I. INTRODUCTION

The goal of inertial confinement fusion (ICF)^{1–3} is to implode a spherical target to achieve high compression of the deuterium-tritium (DT) fuel and high temperature in the hot spot to trigger ignition and produce significant thermonuclear energy gain. Hydrodynamic instabilities and mix play a central role in the performance degradation of spherical implosions in ICF.^{2,3} In indirect-drive ICF implosion experiments at the National Ignition Facility (NIF),⁴ the laser drive was converted into x rays inside a high-Z enclosure (hohlraum) to drive the spherical plastic capsules containing layered DT fuel layers.^{2,3} The implosion begins with an acceleration phase when the x-rays ablate the shell surface, and the capsule accelerates and starts to converge. Outer-shell nonuniformities grow as a result of the acceleration-phase Richtmyer-Meshkov (RM)^{5,6} and Rayleigh–Taylor (RT) instabilities^{7,8} at this stage of the implosion.^{9–29} As the shell accelerates, these outer-surface perturbations feed

through the shell, seeding perturbations on the ablator-ice interface and the inner-ice surface.^{2,3} At this time, ablator jets from localized surface perturbations can penetrate the shell and mix ablator material into the DT hot spot.³⁰ As the shell approaches its center, it starts to decelerate due to rising inner gas pressure while continuing to converge. At stagnation, the shell stops (at peak compression) and then rebounds. During the deceleration phase, the inner surface of the shell is subjected to hydrodynamic instabilities.^{31–38} At this phase, drive asymmetries and surface imperfections are further amplified by the instabilities resulting in a distorted shell with reduced hot-spot temperature, increased volume, and decreased pressure.³⁹ The modulations also grow due to Bell–Plesset (BP) convergence effects throughout the compression.⁴⁰

In recent high-compression experiments on NIF, high fuel areal densities (up to ~ 1.3 g/cm²) have been achieved with fuel velocities of ~ 320 – 330 km/s.^{39,41} These key performance parameters were close to the goal of the ignition design, while the neutron yields were reduced by hydrodynamic instabilities and drive asymmetries.^{39,41} The presence of mixed ablator material was also correlated with reduced experimental yields and temperatures in high-compression

^{a)}Paper QI3 3, *Bull. Am. Phys. Soc.* **58**, 279 (2013).

^{b)}Invited speaker.

layered DT implosions.^{42,43} The x-ray spectroscopy measurements with Cu and Ge dopants at different radial locations in the plastic ablator indicate that the ablation-front instability is primarily responsible for the hot spot mix, not the classical Rayleigh-Taylor hydrodynamic instability at the ablator/DT-ice interface during the acceleration phase.⁴² Multidimensional (2D and 3D) simulations of the layered DT implosions attempted to capture performance degradation due to instabilities and drive asymmetries. They over-predicted the measured yields by factors of up to ~ 30 for high-compression implosions.⁴⁴ 2D simulations with multipliers (up to $3\text{--}5\times$) on the capsule surface roughness, however, were able to bring simulated yields down to the measured levels.⁴¹ The need for an increased surface roughness could indicate the presence of instability seeds, which are not measured by current techniques, or growth rates that are larger than calculated. These results demonstrated a need to quantitatively understand the instability growth in experiments and simulations before a strategy to mitigate them can be designed for high-compression implosions.

Several experimental platforms are being developed to measure and understand various aspects of the instability growth and mix in ignition-relevant conditions on NIF. They include experiments to measure instabilities in both the acceleration and deceleration phases of implosions, at both the outer-ablator and ablator-ice interfaces using various experimental techniques including x-ray imaging, x-ray spectroscopy, and nuclear techniques. This article reviews experimental results from two campaigns that measured instability growth at the ablation surface in the acceleration phase⁴⁵ and at the shell-gas interface in the deceleration phase of plastic-shell implosions.⁴⁶ The ablation-front instability experiments are described in Sec. II. The atomic-mix experiments near peak compression of the plastic-shell implosions are discussed in Sec. III. The discussion of the results is presented in Sec. IV and summarized in Sec. V.

II. ABLATION-FRONT INSTABILITY EXPERIMENTS

Rayleigh-Taylor growth experiments were designed to measure instability at the acceleration phase of spherical implosions⁴⁵ at National Ignition Facility.⁴ Figure 1 shows the experimental configuration including the Au hohlraum, plastic (CH) capsule, Au cone, and the vanadium backlighter. The gold cone provided a possibility for the backlighter x-rays to pass through a single wall of the shell, enabling high-quality

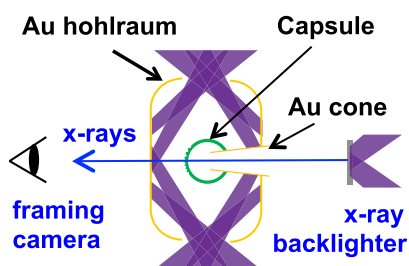


FIG. 1. Experimental configuration schematically shows the target including Au hohlraum, plastic (CH) capsule, Au cone, and the vanadium backlighter. The gold cone provided a possibility for the backlighter x-rays to pass through a single wall of the shell.

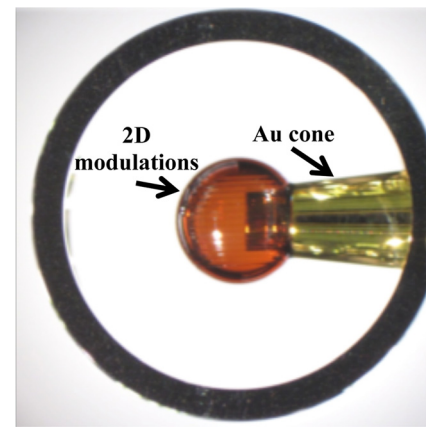


FIG. 2. A picture of the capsule with pre-imposed 2D modulations and a gold cone oriented along a diagnostic line of sight. The outer circular feature is the equatorial diagnostic band before hohlraum assembly.

radiographs of the growing modulations. The experimental configuration was similar to previous backlighting experiments on NIF.⁴⁷ The differences included the additional gold cone, the backlighter material (vanadium vs. germanium), and the reduced thickness ($80\ \mu\text{m}$ vs. $160\ \mu\text{m}$) of the high-density carbon (HDC) window placed at the hohlraum wall. Figure 2 shows an image of the capsule and the gold cone used in these experiments. The capsules had pre-imposed, 2D sinusoidal modulations at three wavelengths, $240\ \mu\text{m}$ (mode 30), $120\ \mu\text{m}$ (mode 60), and $80\ \mu\text{m}$ (mode 90). The initial modulation amplitudes were in the range from $0.25\ \mu\text{m}$ to $1.7\ \mu\text{m}$. The experiments were driven with a shaped, 21-ns long laser pulse with peak power of $\sim 350\ \text{TW}$ and total laser energy of $1.3\ \text{MJ}$ (shown in Fig. 3) using 184 beams of the NIF laser system. An additional eight overlapped beams were used to drive a $12.5\ \mu\text{m}$ thick vanadium backlighter foil at peak laser intensity of $\sim 5 \times 10^{14}\ \text{W}/\text{cm}^2$. The experiments were conducted with the drives and conditions similar to those used in high-compression layered DT implosions.⁴¹ They were designed to test the hydrodynamic growth predictions used to model these DT layered implosions that achieved fuel areal densities of $\sim 1.3\ \text{g}/\text{cm}^2$, peak fuel velocities of $\sim 320\text{--}330\ \text{km}/\text{s}$, and driven at peak

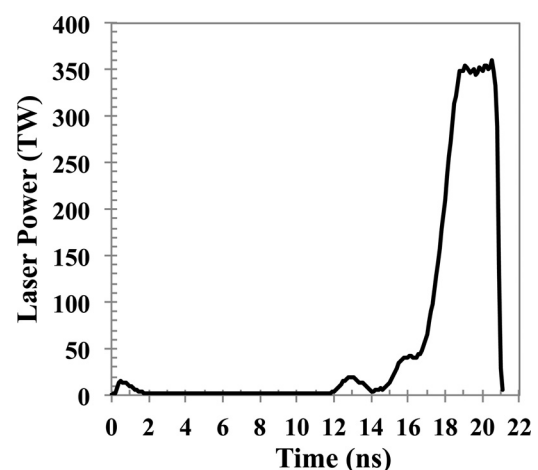


FIG. 3. The laser pulse shape used in the experiments for hohlraum drive had a peak power of $\sim 350\ \text{TW}$ and total energy of $\sim 1.3\ \text{MJ}$.

radiation temperatures of ~ 300 eV.⁴¹ The nominal $209\ \mu\text{m}$ thick plastic capsules with nominal $1120\ \mu\text{m}$ outer radii had the similar Si-doped layers as used in the previous DT layered implosion, as previously published in Ref. 41. An extra $14\ \mu\text{m}$ thick CH layer was used to replace the $69\ \mu\text{m}$ thick DT layer to maintain the similar shell mass as in the layered DT implosions. Current experiments followed a campaign that characterized the implosion shock timing and symmetry.^{38,48,49}

The modulation growth was measured with through-foil x-ray radiography²⁶ using ~ 5.4 -keV x-rays generated by the vanadium backlighter located 12 mm from the target center.⁴⁵ Figure 4 shows capsule x-ray radiographs captured on a framing camera. The central four images of growing capsule modulations were formed using $20\ \mu\text{m}$ wide slit, while images on the right and left sides of the slit images were formed with $20\ \mu\text{m}$ and $50\ \mu\text{m}$ pinholes. This experiment was performed with side-by-side mode 60 and mode 90 modulations. The temporal resolution of the framing camera was 100 ps, while spatial resolution of the slit images was $20\ \mu\text{m}$. The slit and pinholes were positioned 100 mm from the target center, while the detector, a framing camera,⁵⁰ was located 1300 mm from the target center, giving a magnification of ~ 12 for the imaging system. Pinhole images on the right-hand-side of the Fig. 4 included a section attenuated by a $30\ \mu\text{m}$ aluminum strip, used to measure the sensitivity of the system. X-ray filters used in these experiments included $150\ \mu\text{m}$ polyimide and $12.5\ \mu\text{m}$ thick vanadium filters. The measurements were conducted for convergence ratios up to ~ 2 , where the shell radius was decreased down to $\sim 550\ \mu\text{m}$ in the implosions. Optical-depth (OD) variations (used in the analysis below) were obtained by taking a natural logarithm of the framing-camera images after x-ray backgrounds were subtracted.

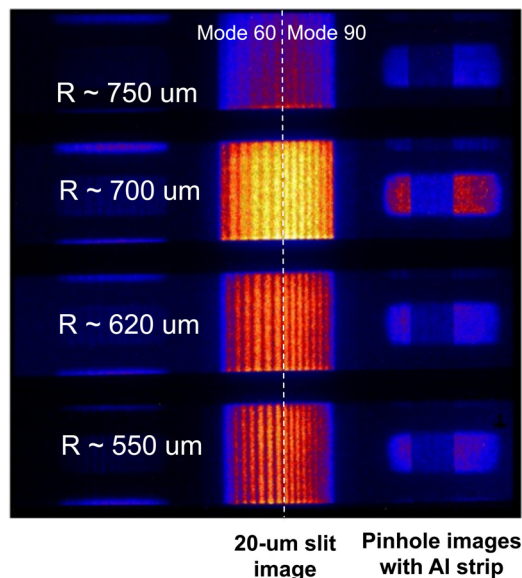


FIG. 4. Measured capsule x-ray radiographs captured on a framing camera. The central four images were formed using a $20\ \mu\text{m}$ wide slit, while images on the right and left sides of the slit images were formed with $20\ \mu\text{m}$ and $50\ \mu\text{m}$ pinholes. This experiment was performed with side-by-side mode 60 (initial wavelength of $120\ \mu\text{m}$) and mode 90 (initial wavelength of $80\ \mu\text{m}$) modulations.

Figure 5 shows measured optical-depth modulation growth for modes 30 [Fig. 5(a)], 60 [Fig. 5(b)], and 90 [Fig. 5(c)] as a function of the modulation wavelength. As the capsule implodes, the wavelengths of the modulations decrease while the modulation amplitudes increase, so the time increases from the right to left in Fig. 5. The results are compared with simulation predictions post-processed using 5.4-keV backlighter energy, 100-ps temporal resolution, and $20\ \mu\text{m}$ spatial resolution. The measured growth was in good agreement with that predicted for all three modes. Since the wavelength is a measure of the radius, the good agreement between simulations and experiments indicates not only a good modeling of the modulation growth but also indicates a good modeling of the implosion itself. Figure 6 shows measured and calculated modulation OD growth factors as a function of the modulation mode number at a shell radius of $650\ \mu\text{m}$, corresponding to a measurement time of 20.3 ns. The OD growth factor was defined as the ratio of the modulation OD amplitude at the time of the measurement to the initial modulation OD amplitude. Effects of the spatial

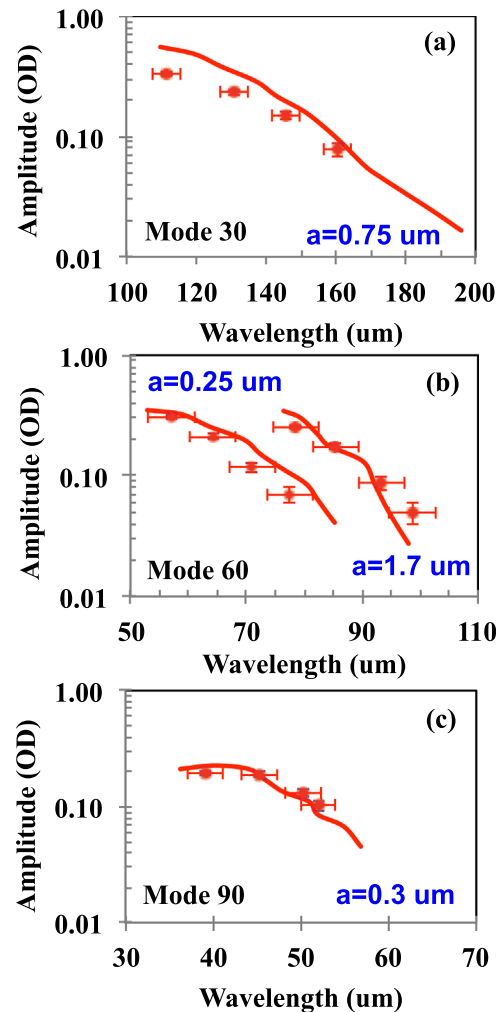


FIG. 5. Evolution of the measured (symbols) and simulated (solid curves) amplitudes of the optical-depth modulations as a function of measured modulation wavelength for (a) mode 30 with initial wavelength of $240\ \mu\text{m}$ and amplitude of $0.75\ \mu\text{m}$, (b) mode 60 with initial wavelength of $120\ \mu\text{m}$ and amplitudes of 1.7 and $0.25\ \mu\text{m}$, and (c) mode 90 with initial wavelength of $80\ \mu\text{m}$ and amplitude of $0.3\ \mu\text{m}$.

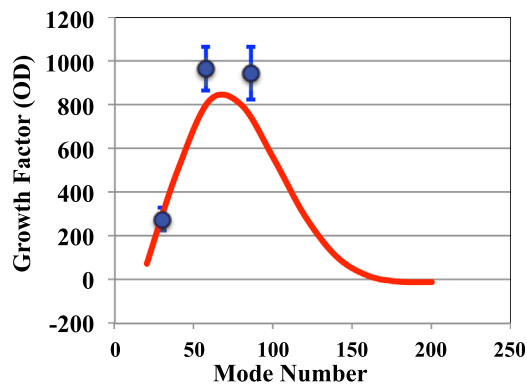


FIG. 6. Measured (symbols) and calculated (solid curve) growth factors for optical-depth modulations as a function of the modulation mode number are shown at a shell radius of $650\ \mu\text{m}$, corresponding to a measurement time of 20.3 ns.

resolution were taken out in the measured experimental points for fair comparison. The good agreement between simulations and experiments indicated that instability growth was modeled well for the most unstable modulations in the high-convergence layered DT implosions in the acceleration phase at convergence ratios up to ~ 2 .

III. DECELERATION-PHASE MIX EXPERIMENTS

Figure 7 schematically shows two types of capsules used in the atomic-mix spherical implosion experiments.⁴⁶ Plastic shells had nominal $209\ \mu\text{m}$ thicknesses and $2280\ \mu\text{m}$ -initial outer diameters. Si-doped layers were used to reduce preheat of the inner CH ablator from M-band emission from the Au hohlraum wall. In the first type of capsules, plastic shells included carbon-deuterium (CD) layers with $4.0\ \mu\text{m}$ thicknesses, placed at either the inner shell surface, or offset by up to $8.0\ \mu\text{m}$ from the inner surface, as shown in Fig. 7(a). The capsules were filled with high-purity tritium gas (including a small contamination of deuterium gas of 0.1% by atom fraction) to allow shell-gas atomic mix to be studied using the DT fusion reaction ($\text{D} + \text{T} \rightarrow {}^4\text{He} + \text{n}$) by measuring the DT neutron yield and ion temperature. The

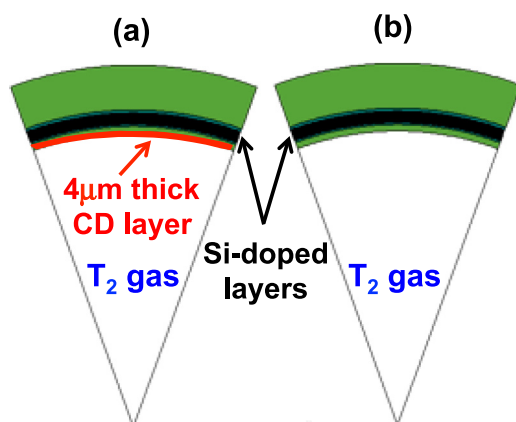


FIG. 7. Capsule schematics (a) with $4\ \mu\text{m}$ thick CD layer and (b) without CD layer (“CH capsules”). The CD layer was placed either at the inner shell surface, or recessed from the inner surface by 1.2, 2.3, 3.9, and $8.0\ \mu\text{m}$ of CH layers. The capsules were filled with tritium gas with mass density of $11.05\ \text{mg/cc}$ at temperature of 32 K.

background DT yields from this D contamination were measured in additional control implosions that did not contain the CD layers (“CH capsules”), as shown in Fig. 7(b). The DT reactions from these control implosions were also used as a diagnostic of the central core ion temperature. The results presented in this article describe shell-gas atomic mix generated at the inner shell-gas interface by the classical RT instability^{2,3} (with no ablative stabilization) in the deceleration phase of implosions, while previous data^{42,43} were collected in layered DT implosions, where ablator mix in the DT hot spot was driven at the outer ablation surface by the ablative RT instability in the acceleration phase of implosions.

All implosions used a laser pulse with peak power of $\sim 435\ \text{TW}$ and total laser energy of $\sim 1.5\ \text{MJ}$ (shown in Fig. 8); the same pulse was used in a number of cryogenic layered DT implosions.⁴⁹ Details of the laser pulse shape, pointing, and hohlraum geometry were determined in previous experiments as described in Ref. 49. The capsule and drive parameters were kept very similar in this set of experiments. Capsule thickness and outer diameter varied less than 0.5% and 1.5%, respectively. The laser power profiles were identical to the $\sim 5\%$ level. The performance of all implosions was characterized with a comprehensive set of nuclear and x-ray diagnostics.⁴⁶ The x-ray fluxes of hohlraum radiation from the laser entrance hole were measured with the Dante diagnostic;⁴⁹ the inferred x-ray flux temperatures were very repeatable, $T_r = 294 \pm 4\ \text{eV}$ in all shots. Measured implosion x-ray bang times were $\sim 22.55 \pm 0.10\ \text{ns}$, all within 100 ps from each other, with the burn width $\sim 300\ \text{ps}$ in all shots.

Figure 9 shows an example of the measured neutron spectrum in one of the “CH capsule” implosions without a CD layer.^{46,51} The peak at 14.1 MeV was used to measure both the total DT neutron yield and the ion temperature in the DT producing region, while neutrons below 9 MeV were used to measure the tritium-tritium (TT) yield in the central hot spot. Target compression was inferred using the down-scattered ratio⁵² (DSR $\sim 1.2\%$) of scattered neutrons in the range from 10 to 12 MeV, relative to primary neutrons in the range from 13 to 15 MeV.⁴⁶ The convergence ratio of ~ 15 ,

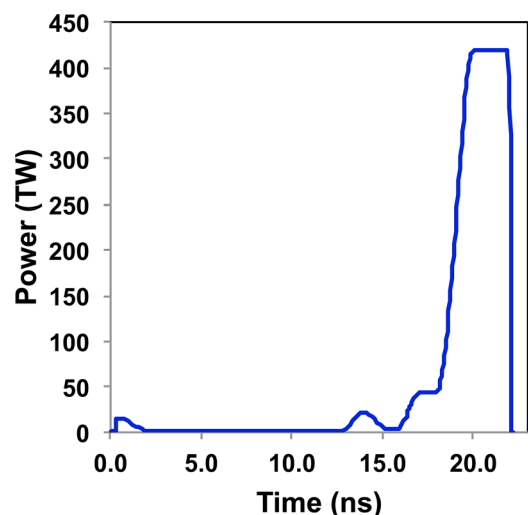


FIG. 8. Laser pulse shape used in the experiments with peak power of $\sim 436\ \text{TW}$ and total energy of $\sim 1.5\ \text{MJ}$.

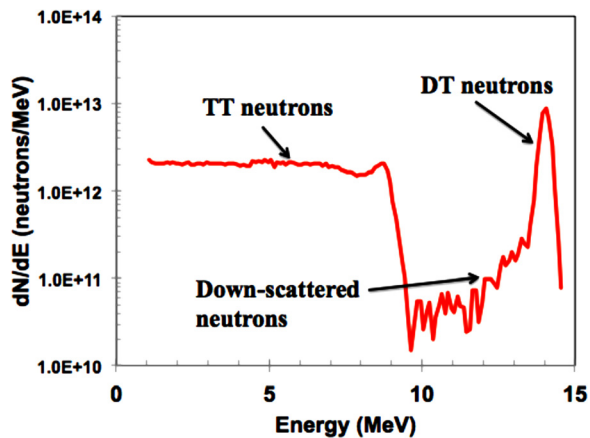


FIG. 9. Measured neutron spectrum for “CH capsule” implosion without CD layer showing DT neutron peak at ~ 14 MeV, down-scattered neutron region between 10 and 12 MeV, and TT neutron region below 9 MeV.

defined as the ratio of the initial inner-capsule radius to the hot spot radius at peak burn, was measured in these implosion using x-ray imaging.⁴⁶ Figure 10 shows the measured neutron diagnostic results and comparisons with ARES simulations.⁵³ The DT yields, DT ion temperatures, and TT yields are shown in Figs. 10(a)–10(c), respectively. In

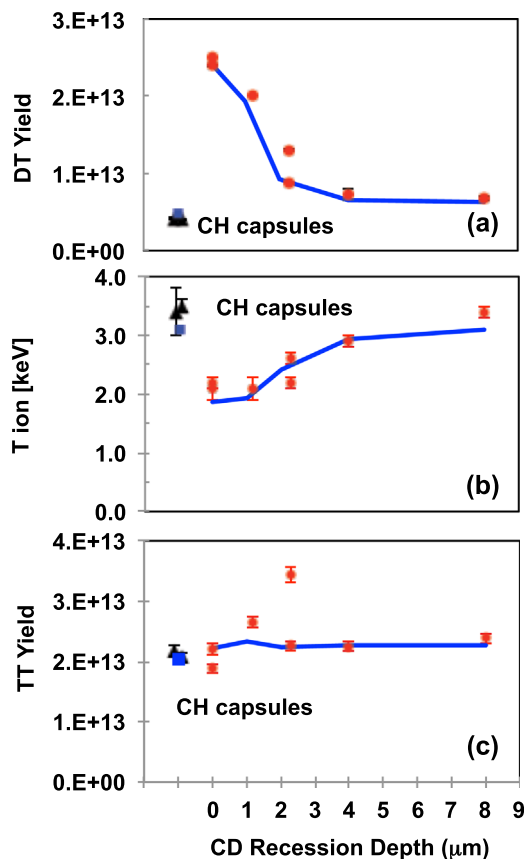


FIG. 10. Measured and simulated (a) DT neutron yield, (b) the ion temperature inferred from the time-of-flight broadening of the DT fusion yields, and (c) TT neutron yield, as a function of recession depth of the CD layer, and for CH capsules without a CD layer. Also shown are results of 2D ARES simulations including a K-L mix model, with initial turbulent mixing length of $L_0 = 0.1$ nm (solid curve). The blue curves represent simulations of the CH capsules. The measurements are shown by the red solid symbols.

implosions without CD layers (labeled “CH capsules”), the measured TT and DT yields along with DT ion temperatures probed the same conditions in the central part of the core. In implosions with CD layers, the DT yields were up to ~ 6 times higher, and DT ion temperatures were lower (~ 2.0 keV vs. 3.4 keV), compared to “CH capsules.” The lower measured temperature supports the hypothesis that the DT neutrons were primarily generated in the colder region near the shell-gas interface where D and T were atomically mixed. As the recession of the CD layers from the inner surface increased, the measured DT yields decreased, indicating that much of the plastic mixed into the gas came from a region close to the inner surface. The TT yields were similar in all implosions with and without CD layers, indication of excellent experimental repeatability.

The experimental results were also compared with 2D simulations using the code ARES.⁵³ To capture the dominant ablation-front instability growth with mode numbers $l < \sim 100$, direct numerical simulations were performed with imposed surface roughness at unstable interfaces. The K-L mix model⁵⁴ (where K represents turbulent kinetic energy, and L is the spatial scale of the mixing layer) was included to capture the turbulent regime and the effects of mix at scales smaller than the computational grid. The free parameter in this method was the initial turbulent mixing length, L_0 , set at all unstable interfaces. As shown in Fig. 10, the simulations match well the whole set of experiments. For this, a multiplier of 3 times on the nominal outer surface roughness was required to match the measured conditions in the central hot core, as determined by the TT yield. The measured outer surface roughness in these experiments varied from 0.5 to almost 2 times the nominal value; thus, the $3\times$ nominal values needed to match the TT yield represent up to a factor of ~ 6 above the measured roughness. This need for a multiplier is consistent with previous 2D simulations of high-compression layered DT implosions.⁴⁴ To explain the conditions in outer colder core (DT yield and ion temperature), a low roughness parameter of $L_0 = 0.1$ nm was used in the K-L mix model. These results indicated that the low-mode hydrodynamic instabilities due to surface non-uniformities were the primary reason for yield degradation with atomic ablator-gas mix playing a secondary role. The measured ion temperature of ~ 3.4 keV for the CD layer recession of $8.0 \mu\text{m}$ was similar to that for the “CH capsules” without CD layers, while the measured DT yield for the $8.0 \mu\text{m}$ recessed layer was slightly larger ($\sim 40\%$) than that for the “CH capsules.” The increased yield was consistent with measured deuterium contamination of tritium gas for the $8.0 \mu\text{m}$ recessed shot that was about 40% larger than for the “CH capsule” shots. This indicated that contributions of the mixed CD to the measured ion temperature and DT yield were small compared to levels set by deuterium contamination in the $8.0 \mu\text{m}$ recessed CD layer shot.

IV. DISCUSSION

In recent high-compression experiments on NIF, a fuel areal density of $\sim 1.3 \text{ g/cm}^2$ has been achieved with a fuel velocity of $\sim 320\text{--}330 \text{ km/s}$.⁴⁵ While these two key performance

parameters were close to the ignition goals, the neutron yield was significantly lower than predicted.⁴⁴ Original multidimensional simulations of the layered DT, high-compression implosions intending to capture performance degradation due to instabilities and drive asymmetries over-predicted measured yields by factors of ~ 5 to ~ 30 .⁴⁴ Two-dimensional simulations with large multipliers (up to $\sim 5\times$) on the capsule surface roughness could bring simulated yields down to the measured levels.⁴⁴ This prompted the hypothesis that the instability growth factors were larger than in simulations.

As shown in Sec. III, the implosion experiments using plastic capsules with CD layers and filled tritium gas measured performance of lower-convergence (compared to layered DT) implosions and directly measured ablator atomic mix using the DT nuclear reaction. Two-dimensional simulations of these experiments,⁴⁴ which included the turbulent K-L mix model⁵⁴ to capture the effects of high-mode mix, could explain the experimental results, but still required large surface roughness multipliers, consistent with modeling of high-compression layered DT implosions. These atomic-mix experiments suggested that hydrodynamic instabilities (with Legendre mode numbers $l < 100$) were the primary cause of yield degradation, with atomic ablator-gas mix playing a secondary role.

There were several possible explanations for the need for large multipliers on the initial surface perturbation. The effective roughness could have been larger than assumed based on current metrology methods. The Rayleigh-Taylor^{7,8} growth rates during the acceleration phase, or the pre-acceleration amplitudes established during the Richtmyer-Meshkov^{5,6} instability phase could also be larger than simulated. Some possible seeds for instability growth, such as radiation asymmetry,⁵⁵ dust grains and other localized defects, and the effect of the membrane (“tent”) used to support the capsule^{56,57} were not included or were underestimated in the simulations. The resultant elevated modulations could cause stronger performance degradation at peak compression, as suggested in recent simulations.⁵⁸ In order to explain past results and inform future designs, predictions of hydrodynamic instability growth needed to be tested and validated by experiments.

As shown in Sec. II, the first experiments to directly measure ablation-front hydrodynamic growth using x-ray radiography of pre-imposed, 2D sinusoidal perturbations were performed at NIF. The goal was to test hydrodynamic growth in simulations during both the Richtmyer-Meshkov phase and the Rayleigh-Taylor phase at the outer ablation surface with moderate capsule convergence (2–3). The measured growth was in good agreement with that predicted, thus validating simulations for the fastest growing modulations with mode numbers up to 90 in the acceleration phase. These results provide confidence in the predictive capability of calculations that are used to define a path toward ignition.

Recent, fully integrated, 2D and 3D simulations generally were unable to fully include the effects of ablator jets in the DT fuel,⁵⁸ but the presence of mixed ablator material was correlated with reduced experimental yields and temperatures in the high-compression layered DT implosions.^{42,43} This supported another hypothesis that ablator jet mix³⁰ was

also a major contributor to yield degradation. Future radiography experiments are planned to address this physics by measuring growth factors of high-mode modulations, representative of the modulations that can produce ablator jets into the DT hot spot. In addition, the ablation-front radiography measurements will be extended to the time of peak shell velocity, testing code predictions of the ablation-surface growth simulation up to the end of acceleration phase at convergence ratios up to ~ 5 . They will be conducted with 3D modulations representative of the surface roughness and imperfections in the recent layered DT implosions. Additional experiments are also planned to measure modulation growth and jet-related mix in the deceleration phase with pre-imposed 2D, 3D modulations, and with spectroscopic layers, extending previous time-integrated mix measurements^{42,43} including a capability of temporal resolution of the mix and also better spatial resolution.

V. CONCLUSIONS

Hydrodynamic instability growth and its effects on implosion performance and mix were studied at the National Ignition Facility. The results of atomic-mix experiments using plastic shells with CD layers have indicated that the hydrodynamic instabilities due to surface roughness (with Legendre mode numbers $l < 100$) were the primary culprits to yield degradation in plastic shell implosions, with atomic ablator-gas mix playing a secondary role. Hydrodynamic instability growth measurements with pre-imposed modulations were performed to test predictions of the ablation-front Rayleigh-Taylor unstable growth in implosions with convergence ratio of ~ 2 . The measured growth was in good agreement with that predicted, thus validating simulations for the fastest growing modulations with mode numbers up to 90 in the acceleration phase. Future acceleration-phase instability experiments will be extended to shorter wavelengths and to higher convergence ratios up to ~ 5 . In addition, deceleration phase instability experiments are also planned to test and validate simulation predictions near peak compression of the spherical implosions.

ACKNOWLEDGMENTS

This work was performed under the auspices of the U.S. Department of Energy by Lawrence Livermore National Laboratory under Contract No. DE-AC52-07NA27344.

¹J. Nuckolls, L. Wood, A. Thiessen, and G. Zimmerman, *Nature* **239**, 139 (1972).

²S. Atzeni and J. Meyer-ter-Vehn, *The Physics of Inertial Fusion: Beam Plasma Interaction, Hydrodynamics, Hot Dense Matter*, International Series of Monographs on Physics (Clarendon Press, Oxford, 2004).

³J. D. Lindl, *Inertial Confinement Fusion: The Quest for Ignition and Energy Gain Using Indirect Drive* (Springer-Verlag, New York, 1998).

⁴E. I. Moses, R. N. Boyd, B. A. Remington, C. J. Keane, and R. Al-Ayat, *Phys. Plasmas* **16**, 041006 (2009); G. H. Miller, E. I. Moses, and C. R. Wuest, *Opt. Eng.* **43**, 2841 (2004).

⁵R. D. Richtmyer, *Commun. Pure Appl. Math.* **13**, 297 (1960).

⁶E. E. Meshkov, *Izv. Acad. Sci. USSR Fluid Dyn.* **4**, 101 (1969).

⁷Lord Rayleigh, *Proc. London Math Soc.* **XIV**, 170 (1883).

⁸G. Taylor, *Proc. R. Soc. London, Ser. A* **201**, 192 (1950).

- ⁹S. G. Glendinning, S. N. Dixit, B. A. Hammel, D. H. Kalantar, M. H. Key, J. D. Kilkenny, J. P. Knauer, D. M. Pennington, B. A. Remington, R. J. Wallace, and S. V. Weber, *Phys. Rev. Lett.* **78**, 3318 (1997).
- ¹⁰K. S. Budil, B. A. Remington, T. A. Peyser, K. O. Mikaelian, P. L. Miller, N. C. Woolsey, W. M. Wood-Vasey, and A. M. Rubenchik, *Phys. Rev. Lett.* **76**, 4536 (1996).
- ¹¹K. S. Budil, B. Lasinski, M. J. Edwards, A. S. Wan, B. A. Remington, S. V. Weber, S. G. Glendinning, L. Suter, and P. E. Stry, *Phys. Plasmas* **8**, 2344 (2001).
- ¹²B. A. Remington, S. V. Weber, M. M. Marinak, S. W. Haan, J. D. Kilkenny, R. Wallace, and G. Dimonte, *Phys. Rev. Lett.* **73**, 545 (1994).
- ¹³M. M. Marinak, S. G. Glendinning, R. J. Wallace, B. A. Remington, K. S. Budil, S. W. Haan, R. E. Tipton, and J. D. Kilkenny, *Phys. Rev. Lett.* **80**, 4426 (1998).
- ¹⁴J. Grun, M. E. Emery, C. K. Manka, T. N. Lee, E. A. McLean, A. Mostovych, J. Stamper, S. Bodner, S. P. Obenschain, and B. H. Ripin, *Phys. Rev. Lett.* **58**, 2672 (1987).
- ¹⁵K. Shigemori, H. Azechi, M. Nakai, M. Honda, K. Meguro, N. Miyanaga, H. Takabe, and K. Mimi, *Phys. Rev. Lett.* **78**, 250 (1997).
- ¹⁶J. P. Knauer, R. Betti, D. K. Bradley, T. R. Boehly, T. J. B. Collins, V. N. Goncharov, P. W. McKenty, D. D. Meyerhofer, V. A. Smalyuk, C. P. Verdon, S. G. Glendinning, D. H. Kalantar, and R. G. Watt, *Phys. Plasmas* **7**, 338 (2000).
- ¹⁷R. J. Taylor, J. P. Dahlburg, A. Iwase, J. H. Gardner, D. E. Fyfe, and O. Willi, *Phys. Rev. Lett.* **76**, 1643 (1996).
- ¹⁸D. H. Kalantar, M. H. Key, L. B. Da Silva, S. G. Glendinning, B. A. Remington, J. E. Rothenberg, F. Weber, S. V. Weber, E. Wolftrum, N. S. Kim, D. Neely, J. Zhang, J. S. Wark, A. Demir, J. Lin, R. Smith, G. J. Tallents, C. L. S. Lewis, A. MacPhee, J. Warwick, and J. P. Knauer, *Phys. Plasmas* **4**, 1985 (1997).
- ¹⁹H. Azechi, M. Nakai, K. Shigemori, N. Miyanaga, H. Shiraga, H. Nishimura, M. Honda, R. Ishizaki, J. G. Wouchuk, H. Takabe, K. Nishihara, K. Mima, A. Nishiguchi, and T. Endo, *Phys. Plasmas* **4**, 4079 (1997).
- ²⁰C. J. Pawley, S. E. Bodner, J. P. Dahlburg, S. P. Obenschain, A. J. Schmitt, J. D. Sethian, C. A. Sullivan, J. H. Gardner, Y. Aglitskiy, Y. Chan, and T. Lehecka, *Phys. Plasmas* **6**, 565 (1999).
- ²¹V. A. Smalyuk, T. R. Boehly, D. K. Bradley, V. N. Goncharov, J. A. Delettrez, J. P. Knauer, D. D. Meyerhofer, D. Oron, and D. Shvarts, *Phys. Rev. Lett.* **81**, 5342 (1998).
- ²²T. R. Boehly, V. N. Goncharov, O. Gotchev, J. P. Knauer, D. D. Meyerhofer, D. Oron, S. P. Regan, Y. Srebro, W. Seka, D. Shvarts, S. Skupsky, and V. A. Smalyuk, *Phys. Plasmas* **8**, 2331 (2001).
- ²³V. A. Smalyuk, O. Sadot, J. A. Delettrez, D. D. Meyerhofer, S. P. Regan, and T. C. Sangster, *Phys. Rev. Lett.* **95**, 215001 (2005).
- ²⁴V. A. Smalyuk, O. Sadot, R. Betti, V. N. Goncharov, J. A. Delettrez, D. D. Meyerhofer, S. P. Regan, T. C. Sangster, and D. Shvarts, *Phys. Plasmas* **13**, 056312 (2006).
- ²⁵O. Sadot, V. A. Smalyuk, J. A. Delettrez, D. D. Meyerhofer, T. C. Sangster, R. Betti, V. N. Goncharov, and D. Shvarts, *Phys. Rev. Lett.* **95**, 265001 (2005).
- ²⁶V. A. Smalyuk, S. X. Hu, J. Hager, J. A. Delettrez, D. D. Meyerhofer, T. C. Sangster, and D. Shvarts, *Phys. Rev. Lett.* **103**, 105001 (2009).
- ²⁷L. Masse, *Phys. Rev. Lett.* **98**, 245001 (2007).
- ²⁸A. Casner, D. Galmiche, G. Huser, J.-P. Jadaud, S. Liberatore, and M. Vandenboomgaerde, *Phys. Plasmas* **16**, 092701 (2009).
- ²⁹G. Huser, A. Casner, L. Masse, S. Liberatore, D. Galmiche, L. Jacquet, and M. Theobald, *Phys. Plasmas* **18**, 012706 (2011).
- ³⁰B. A. Hammel, H. A. Scott, S. P. Regan, C. Cerjan, D. S. Clark, M. J. Edwards, R. Epstein, S. H. Glenzer, S. W. Haan, N. Izumi, J. A. Koch, G. A. Kyrala, O. L. Landen, S. H. Langer, K. Peterson, V. A. Smalyuk, L. J. Suter, and D. C. Wilson, *Phys. Plasmas* **18**, 056310 (2011).
- ³¹H. Sakagami and K. Nishihara, *Phys. Rev. Lett.* **65**, 432 (1990).
- ³²R. P. J. Town and A. R. Bell, *Phys. Rev. Lett.* **67**, 1863 (1991).
- ³³M. M. Marinak, R. E. Tipton, O. L. Landen, T. J. Murphy, P. Amendt, S. W. Haan, S. P. Hatchett, C. J. Keane, R. McEachern, and R. Wallace, *Phys. Plasmas* **3**, 2070 (1996).
- ³⁴V. Lobatchev and R. Betti, *Phys. Rev. Lett.* **85**, 4522 (2000).
- ³⁵M. C. Herrmann, M. Tabak, and J. D. Lindl, *Phys. Plasmas* **8**, 2296 (2001).
- ³⁶V. A. Smalyuk, V. N. Goncharov, J. A. Delettrez, F. J. Marshall, D. D. Meyerhofer, S. P. Regan, and B. Yaakobi, *Phys. Rev. Lett.* **87**, 155002 (2001).
- ³⁷R. Betti, K. Anderson, V. N. Goncharov, R. L. McCrory, D. D. Meyerhofer, S. Skupsky, and R. P. J. Town, *Phys. Plasmas* **9**, 2277 (2002).
- ³⁸V. A. Smalyuk, J. A. Delettrez, V. N. Goncharov, F. J. Marshall, D. D. Meyerhofer, S. P. Regan, T. C. Sangster, R. P. J. Town, and B. Yaakobi, *Phys. Plasmas* **9**, 2738 (2002).
- ³⁹M. J. Edwards, P. K. Patel, J. D. Lindl, L. J. Atherton, S. H. Glenzer, S. W. Haan, J. D. Kilkenny, O. L. Landen, E. I. Moses, A. Nikroo, R. Petrasso, T. C. Sangster, P. T. Springer, S. Batha, R. Benedetti, L. Bernstein, R. Betti, D. L. Bleuel, T. R. Boehly, D. K. Bradley, J. A. Caggiano, D. A. Callahan, P. M. Celliers, C. J. Cerjan, K. C. Chen, D. S. Clark, G. W. Collins, E. L. Dewald, L. Divol, S. Dixit, T. Döppner, D. H. Edgell, J. E. Fair, M. Farrell, R. J. Fortner, J. Frenje, M. G. Gatu Johnson, E. Giraldez, V. Yu. Glebov, G. Grim, B. A. Hammel, A. V. Hamza, D. R. Harding, S. P. Hatchett, N. Hein, H. W. Herrmann, D. Hicks, D. E. Hinkel, M. Hoppe, W. W. Hsing, N. Izumi, B. Jacoby, O. S. Jones, D. Kalantar, R. Kauffman, J. L. Kline, J. P. Knauer, J. A. Koch, B. J. Koziolowski, G. Kyrala, K. N. LaFortune, S. Le Pape, R. J. Leeper, R. Lerche, T. Ma, B. J. MacGowan, A. J. MacKinnon, A. MacPhee, E. R. Mapoles, M. M. Marinak, M. Mauldin, P. W. McKenty, M. Meezan, P. A. Michel, J. Milovich, J. D. Moody, M. Moran, D. H. Munro, C. L. Olson, K. Opachich, A. E. Pak, T. Parham, H.-S. Park, J. E. Ralph, S. P. Regan, B. Remington, H. Rinderknecht, H. F. Robey, M. Rosen, S. Ross, J. D. Salmonson, J. Sater, D. H. Schneider, F. H. Séguin, S. M. Sepke, D. A. Shaughnessy, V. A. Smalyuk, B. K. Spears, C. Stoeckl, W. Stoeffl, L. Suter, C. A. Thomas, R. Tommasini, R. P. Town, S. V. Weber, P. J. Wegner, K. Widman, M. Wilke, D. C. Wilson, C. B. Yeamans, and A. Zylstra, *Phys. Plasmas* **20**, 070501 (2013).
- ⁴⁰M. S. Plesset and T. P. Mitchell, *Q. Appl. Math.* **13**, 419 (1956).
- ⁴¹V. A. Smalyuk, T. Döppner, J. L. Kline, T. Ma, H.-S. Park, L. J. Atherton, L. R. Benedetti, R. Bionta, D. Bleuel, E. Bond, D. K. Bradley, J. Caggiano, D. A. Callahan, D. T. Casey, P. M. Celliers, C. J. Cerjan, D. Clark, E. L. Dewald, S. N. Dixit, D. H. Edgell, J. Frenje, M. G. Gatu Johnson, V. Y. Glebov, S. Glenn, G. Grim, S. W. Haan, B. A. Hammel, E. Hartouni, R. Hatarik, S. Hatchett, D. G. Hicks, W. W. Hsing, N. Izumi, O. S. Jones, M. H. Key, S. F. Khan, J. D. Kilkenny, J. Knauer, G. A. Kyrala, O. L. Landen, S. Le Pape, B. J. MacGowan, A. J. MacKinnon, A. G. MacPhee, J. McNaney, N. B. Meezan, J. D. Moody, A. Moore, M. Moran, A. Pak, T. Parham, P. K. Patel, R. Petrasso, J. E. Ralph, S. P. Regan, B. A. Remington, H. F. Robey, J. S. Ross, B. K. Spears, P. T. Springer, L. J. Suter, R. Tommasini, R. P. Town, S. V. Weber, K. Widmann, J. D. Lindl, M. J. Edwards, S. H. Glenzer, and E. I. Moses, *Phys. Rev. Lett.* **111**, 215001 (2013).
- ⁴²S. P. Regan, R. Epstein, B. A. Hammel, L. J. Suter, H. A. Scott, M. A. Barrios, D. K. Bradley, D. A. Callahan, C. Cerjan, G. W. Collins, S. N. Dixit, T. Döppner, M. J. Edwards, D. R. Farley, K. B. Fournier, S. Glenn, S. H. Glenzer, I. E. Golovkin, S. W. Haan, A. Hamza, D. G. Hicks, N. Izumi, O. S. Jones, J. D. Kilkenny, J. L. Kline, G. A. Kyrala, O. L. Landen, T. Ma, J. J. MacFarlane, A. J. MacKinnon, R. C. Mancini, R. L. McCrory, N. B. Meezan, D. D. Meyerhofer, A. Nikroo, H.-S. Park, J. Ralph, B. A. Remington, T. C. Sangster, V. A. Smalyuk, P. T. Springer, and R. P. J. Town, *Phys. Rev. Lett.* **111**, 045001 (2013).
- ⁴³T. Ma, S. V. Weber, N. Izumi, P. T. Springer, P. K. Patel, M. H. Key, L. J. Atherton, L. R. Benedetti, D. K. Bradley, D. A. Callahan, P. M. Celliers, C. J. Cerjan, E. L. Dewald, S. N. Dixit, T. Döppner, D. H. Edgell, S. Glenn, G. Grim, S. W. Haan, B. A. Hammel, D. Hicks, W. W. Hsing, O. S. Jones, S. F. Khan, J. D. Kilkenny, J. L. Kline, G. A. Kyrala, O. L. Landen, S. Le Pape, B. J. MacGowan, A. J. MacKinnon, A. G. MacPhee, N. B. Meezan, J. D. Moody, A. Pak, T. Parham, H.-S. Park, J. E. Ralph, S. P. Regan, B. A. Remington, H. F. Robey, J. S. Ross, B. K. Spears, V. Smalyuk, L. J. Suter, R. Tommasini, R. P. Town, J. D. Lindl, M. J. Edwards, S. H. Glenzer, and E. I. Moses, *Phys. Rev. Lett.* **111**, 085004 (2013).
- ⁴⁴D. S. Clark, D. E. Hinkel, D. C. Eder, O. S. Jones, S. W. Haan, B. A. Hammel, M. M. Marinak, J. L. Milovich, H. F. Robey, L. J. Suter, and R. P. J. Town, *Phys. Plasmas* **20**, 056318 (2013).
- ⁴⁵V. A. Smalyuk, D. T. Casey, D. S. Clark, M. J. Edwards, S. W. Haan, A. Hamza, D. E. Hoover, W. W. Hsing, O. Hurricane, J. D. Kilkenny, J. Kroll, O. L. Landen, A. Moore, A. Nikroo, A. Pak, J. L. Peterson, K. Raman, B. A. Remington, H. F. Robey, S. V. Weber, and K. Widmann, "First measurements of hydrodynamic instability growth in indirectly driven implosions at National Ignition Facility," *Phys. Rev. Lett.* (submitted).
- ⁴⁶V. A. Smalyuk, R. E. Tipton, J. E. Pino, D. T. Casey, G. P. Grim, B. A. Remington, D. P. Rowley, S. V. Weber, M. Barrios, R. Benedetti, D. L. Bleuel, D. K. Bradley, J. A. Caggiano, D. A. Callahan, C. J. Cerjan, D. H. Edgell, M. J. Edwards, J. A. Frenje, M. Gatu-Johnson, V. Y. Glebov, S.

- Glenn, S. W. Haan, A. Hamza, R. Hatarik, W. W. Hsing, N. Izumi, S. Khan, J. D. Kilkenny, J. Kline, J. Knauer, O. L. Landen, T. Ma, J. M. McNaney, M. Mintz, A. Moore, A. Nikroo, A. Pak, T. Parham, R. Petrasso, D. B. Sayre, M. Schneider, R. Tommasini, R. P. Town, K. Widmann, D. C. Wilson, and C. B. Yeamans, "Measurements of ablator-gas mix in indirectly driven implosions at National Ignition Facility," *Phys. Rev. Lett.* **112**, 025002 (2014).
- ⁴⁷D. G. Hicks, N. B. Meezan, E. L. Dewald, A. J. Mackinnon, D. A. Callahan, T. Döppner, L. R. Benedetti, D. K. Bradley, P. M. Celliers, D. S. Clark, S. N. Dixit, E. G. Dzenitis, J. E. Eggert, D. R. Farley, S. M. Glenn, S. H. Glenzer, A. V. Hamza, R. F. Heeter, J. P. Holder, N. Izumi, D. H. Kalantar, S. F. Khan, J. J. Kroll, T. Ma, A. G. MacPhee, J. M. McNaney, J. D. Moody, M. J. Moran, B. R. Nathan, K. P. Opachich, R. R. Prasad, J. E. Ralph, H. F. Robey, J. R. Rygg, J. D. Salmonson, M. B. Schneider, N. Simanovskaia, B. K. Spears, R. Tommasini, K. Widmann, G. W. Collins, O. L. Landen, J. D. Kilkenny, W. W. Hsing, B. J. MacGowan, L. J. Atherton, M. J. Edwards, R. E. Olson, J. A. Frenje, R. D. Petrasso, H. G. Rinderknecht, A. B. Zylstra, J. L. Kline, G. A. Kyrala, and A. Nikroo, *Phys. Plasmas* **19**, 122702 (2012).
- ⁴⁸H. F. Robey, T. R. Boehly, P. M. Celliers, J. H. Eggert, D. Hicks, R. F. Smith, R. Collins, M. W. Bowers, K. G. Krauter, P. S. Datte, D. H. Munro, J. L. Milovich, O. S. Jones, P. A. Michel, C. A. Thomas, R. E. Olson, S. Pollaine, R. P. J. Town, S. Haan, D. Callahan, D. Clark, J. Edwards, J. L. Kline, S. Dixit, M. B. Schneider, E. L. Dewald, K. Widmann, J. D. Moody, T. Döppner, H. B. Radousky, A. Throop, D. Kalantar, P. DiNicola, A. Nikroo, J. J. Kroll, A. V. Hamza, J. B. Horner, S. D. Bhandarkar, E. Dzenitis, E. Alger, E. Giraldez, C. Castro, K. Moreno, C. Haynam, K. N. LaFortune, C. Widmayer, M. Shaw, K. Jancaitis, T. Parham, D. M. Holunga, C. F. Walters, B. Haid, E. R. Mapoles, J. Sater, C. R. Gibson, T. Malsbury, J. Fair, D. Trummer, K. R. Coffee, B. Burr, L. V. Berzins, C. Choate, S. J. Brereton, S. Azevedo, H. Chandrasekaran, D. C. Eder, N. D. Masters, A. C. Fisher, P. A. Sterne, B. K. Young, O. L. Landen, B. M. Van Woutherghem, B. J. MacGowan, J. Atherton, J. D. Lindl, D. D. Meyerhofer, and E. Moses, *Phys. Plasmas* **19**, 042706 (2012); H. F. Robey, P. M. Celliers, J. L. Kline, A. J. Mackinnon, T. R. Boehly, O. L. Landen, J. H. Eggert, D. Hicks, S. Le Pape, D. R. Farley, M. W. Bowers, K. G. Krauter, D. H. Munro, O. S. Jones, J. L. Milovich, D. Clark, B. K. Spears, R. P. J. Town, S. W. Haan, S. Dixit, M. B. Schneider, E. L. Dewald, K. Widmann, J. D. Moody, T. Döppner, H. B. Radousky, A. Nikroo, J. J. Kroll, A. V. Hamza, J. B. Horner, S. D. Bhandarkar, E. Dzenitis, E. Alger, E. Giraldez, C. Castro, K. Moreno, C. Haynam, K. N. LaFortune, C. Widmayer, M. Shaw, K. Jancaitis, T. Parham, D. M. Holunga, C. F. Walters, B. Haid, T. Malsbury, D. Trummer, K. R. Coffee, B. Burr, L. V. Berzins, C. Choate, S. J. Brereton, S. Azevedo, H. Chandrasekaran, B. K. Young, M. J. Edwards, B. M. Van Woutherghem, B. J. MacGowan, J. Atherton, J. D. Lindl, D. D. Meyerhofer, and E. Moses, *Phys. Rev. Lett.* **108**, 215004 (2012).
- ⁴⁹S. H. Glenzer, D. A. Callahan, A. J. MacKinnon, J. L. Kline, G. Grim, E. T. Alger, R. L. Berger, L. A. Bernstein, R. Betti, D. L. Bleuel, T. R. Boehly, D. K. Bradley, S. C. Burkhart, R. Burr, J. A. Caggiano, C. Castro, D. T. Casey, C. Choate, D. S. Clark, P. Celliers, C. J. Cerjan, G. W. Collins, E. L. Dewald, P. DiNicola, J. M. DiNicola, L. Divol, S. Dixit, T. Döppner, R. Dylla-Spears, E. Dzenitis, M. Eckart, G. Erbert, D. Farley, J. Fair, D. Fittinghoff, M. Frank, L. J. A. Frenje, S. Friedrich, D. T. Casey, M. Gatu Johnson, C. Gibson, E. Giraldez, V. Glebov, S. Glenn, N. Guler, S. W. Haan, B. J. Haid, B. A. Hammel, A. V. Hamza, C. A. Haynam, G. M. Heestand, M. Hermann, H. W. Hermann, D. G. Hicks, D. E. Hinkel, J. P. Holder, D. M. Holunda, J. B. Horner, W. W. Hsing, H. Huang, N. Izumi, M. Jackson, O. S. Jones, D. H. Kalantar, R. Kauffman, J. D. Kilkenny, R. K. Kirkwood, J. Klingmann, T. Kohut, J. P. Knauer, J. A. Koch, B. Kozioziemki, G. A. Kyrala, A. L. Kritcher, J. Kroll, K. LaFortune, L. Lagin, O. L. Landen, D. W. Larson, D. LaTray, R. J. Leeper, S. Le Pape, J. D. Lindl, R. Lowe-Webb, T. Ma, J. McNaney, A. G. MacPhee, T. N. Malsbury, E. Mapoles, C. D. Marshall, N. B. Meezan, F. Merrill, P. Michel, J. D. Moody, A. S. Moore, M. Moran, K. A. Moreno, D. H. Munro, B. R. Nathan, A. Nikroo, R. E. Olson, C. D. Orth, A. E. Pak, P. K. Patel, T. Parham, R. Petrasso, J. E. Ralph, H. Rinderknecht, S. P. Regan, H. F. Robey, J. S. Ross, M. D. Rosen, R. Sacks, J. D. Salmonson, R. Saunders, J. Sater, C. Sangster, M. B. Schneider, F. H. Séguin, M. J. Shaw, B. K. Spears, P. T. Springer, W. Stoeffl, L. J. Suter, C. A. Thomas, R. Tommasini, R. P. J. Town, C. Walters, S. Weaver, S. V. Weber, P. J. Wegner, P. K. Whitman, K. Widmann, C. C. Widmayer, C. H. Wilde, D. C. Wilson, B. Van Woutherghem, B. J. MacGowan, L. J. Atherton, M. J. Edwards, and E. I. Moses, *Phys. Plasmas* **19**, 056318 (2012).
- ⁵⁰S. M. Glenn, L. R. Benedetti, D. K. Bradley, B. A. Hammel, N. Izumi, S. F. Khan, G. A. Kyrala, T. Ma, J. L. Milovich, A. E. Pak, V. A. Smalyuk, R. Tommasini, and R. P. J. Town, *Rev. Sci. Instrum.* **83**, 10E119 (2012).
- ⁵¹D. B. Sayre, C. R. Brune, J. A. Caggiano, V. Y. Glebov, R. Hatarik, A. D. Bacher, D. L. Bleuel, D. T. Casey, C. J. Cerjan, M. J. Eckart, R. J. Fortner, J. A. Frenje, S. Friedrich, M. Gatu-Johnson, G. P. Grim, C. Hagmann, J. P. Knauer, J. L. Kline, D. P. McNabb, J. M. McNaney, J. M. Mintz, M. J. Moran, A. Nikroo, T. Phillips, J. E. Pino, B. A. Remington, D. P. Rowley, D. H. Schneider, and V. A. Smalyuk, *Phys. Rev. Lett.* **111**, 052501 (2013).
- ⁵²J. A. Frenje, R. Bionta, E. J. Bond, J. A. Caggiano, D. T. Casey, C. Cerjan, J. Edwards, M. Eckart, D. N. Fittinghoff, S. Friedrich, V. Yu. Glebov, S. Glenzer, G. Grim, S. Haan, R. Hatarik, S. Hatchett, M. Gatu Johnson, O. S. Jones, J. D. Kilkenny, J. P. Knauer, O. Landen, R. Leeper, S. Le Pape, R. Lerche, C. K. Li, A. Mackinnon, J. McNaney, F. E. Merrill, M. Moran, D. H. Munro, T. J. Murphy, R. D. Petrasso, R. Rygg, T. C. Sangster, F. H. Séguin, S. Sepke, B. Spears, P. Springer, C. Stoeckl, and D. C. Wilson, *Nucl. Fusion* **53**, 043014 (2013).
- ⁵³R. M. Darlington, T. L. McAbee, and G. Rodrigue, *Comput. Phys. Commun.* **135**, 58 (2001).
- ⁵⁴G. Dimonte and R. Tipton, *Phys. Fluids* **18**, 085101 (2006).
- ⁵⁵R. H. H. Scott, D. S. Clark, D. K. Bradley, D. A. Callahan, M. J. Edwards, S. W. Haan, M. M. Marinak, R. P. J. Town, P. A. Norreys, and L. J. Suter, *Phys. Rev. Lett.* **110**, 075001 (2013).
- ⁵⁶O. L. Landen, R. Benedetti, D. Bleuel, T. R. Boehly, D. K. Bradley, J. A. Caggiano, D. A. Callahan, P. M. Celliers, C. J. Cerjan, D. Clark, G. W. Collins, E. L. Dewald, S. N. Dixit, T. Döppner, D. Edgell, J. Eggert, D. Farley, J. A. Frenje, V. Glebov, S. M. Glenn, S. H. Glenzer, S. W. Haan, A. Hamza, B. A. Hammel, C. A. Haynam, J. H. Hammer, R. F. Heeter, H. W. Herrmann, D. G. Hicks, D. E. Hinkel, N. Izumi, M. Gatu Johnson, O. S. Jones, D. H. Kalantar, R. L. Kauffman, J. D. Kilkenny, J. L. Kline, J. P. Knauer, J. A. Koch, G. A. Kyrala, K. LaFortune, T. Ma, A. J. Mackinnon, A. J. MacPhee, E. Mapoles, J. L. Milovich, J. D. Moody, N. B. Meezan, P. Michel, A. S. Moore, D. H. Munro, A. Nikroo, R. E. Olson, K. Opachich, A. Pak, T. Parham, P. Patel, H.-S. Park, R. P. Petrasso, J. Ralph, S. P. Regan, B. A. Remington, H. G. Rinderknecht, H. F. Robey, M. D. Rosen, J. S. Ross, J. D. Salmonson, T. C. Sangster, M. B. Schneider, V. Smalyuk, B. K. Spears, P. T. Springer, L. J. Suter, C. A. Thomas, R. P. J. Town, S. V. Weber, P. J. Wegner, D. C. Wilson, K. Widmann, C. Yeamans, A. Zylstra, M. J. Edwards, J. D. Lindl, L. J. Atherton, W. W. Hsing, B. J. MacGowan, B. M. Van Woutherghem, and E. I. Moses, *Plasma Phys. Controlled Fusion* **54**, 124026 (2012).
- ⁵⁷S. W. Haan, J. Atherton, D. S. Clark, B. A. Hammel, D. A. Callahan, C. J. Cerjan, E. L. Dewald, S. Dixit, M. J. Edwards, S. Glenzer, S. P. Hatchett, D. Hicks, O. S. Jones, O. L. Landen, J. D. Lindl, M. M. Marinak, B. J. MacGowan, A. J. Mackinnon, N. B. Meezan, J. L. Milovich, D. H. Munro, H. F. Robey, J. D. Salmonson, B. K. Spears, L. J. Suter, R. P. Town, S. V. Weber, J. L. Kline, and D. C. Wilson, *Fusion Sci. Technol.* **63**, 67 (2013).
- ⁵⁸S. V. Weber, D. T. Casey, J. E. Pino, D. P. Rowley, V. A. Smalyuk, B. K. Spears, and R. E. Tipton, "NIF symmetry capsule modeling," *Bull. Am. Phys. Soc.* **58**, 195 (2013).